

3-D Coordination Polymers Based on the Tetrathiafulvalenetetracarboxylate (TTF-TC) Derivative: Synthesis, Characterization, and Oxidation Issues

Thi Le Anh Nguyen,[†] Rezan Demir-Cakan,[‡] Thomas Devic,^{*,†} Mathieu Morcrette,[‡] Tim Ahnfeldt,[§] Pascale Auban-Senzier,^{||} Norbert Stock,[§] Anne-Marie Goncalves,[†] Yaroslav Filinchuk,[⊥] Jean-Marie Tarascon,[‡] and Gérard Férey[†]

[†]Institut Lavoisier, UMR CNRS 8180, Université de Versailles Saint-Quentin-en-Yvelines, 45 avenue des Etats-Unis, 78035 Versailles cedex, France, [‡]LRCS UMR CNRS 6007, Université de Picardie Jules Verne, 33 rue Saint-Leu, 80039 Amiens, France, [§]Institute of Inorganic Chemistry, Christian-Albrechts-Universität, Otto-Hahn-Platz 6/7, 24118 Kiel, Germany, ^{||}Laboratoire de Physique des Solides, UMR CNRS 8502, Bât. 510, Université de Paris-Sud, 91405 Orsay, France, and [⊥]SNBL at ESRF, 38043 Grenoble, France

Received May 12, 2010

The reactivity of the redox-active tetracarboxylic acid derived from the tetrathiafulvalene (TTF-TC)₄ with alkaline cations (K, Rb, Cs) is reported. The exploration of various experimental parameters (temperature, pH) led to the formation of four crystalline three-dimensional coordination polymers formulated M₂(TTF-TC)H₂ (M = K, Rb, Cs), denoted MIL-132(K), MIL-133(isostructural K, Rb), and MIL-134(Cs). Thermogravimetric analysis and thermodiffraction show that all of the solids are thermally stable up to 150–200 °C in the air. In order to exploit the possibility of oxidation of the organic linker in TTF-based compounds, they were employed as positive electrodes in a classical lithium cell. A highly reversible cyclability was achieved at high current density (10 C) with a reasonable performance (~50 mAh g⁻¹). Finally, combined electro-(sub)hydrothermal synthesis was used to prepare a fifth 3-D coordination polymer formulated K(TTF-TC)H₂ (denoted MIL-135(K)), this time not based on the neutral TTF-TC linker but its radical, oxidized form TTF-TC^{•+}. This solid is less thermally stable than its neutral counterparts but exhibits a semiconducting behavior, with a conductivity at room temperature of about 1 mS cm⁻¹.

Introduction

Among the numerous properties which can be hosted by porous coordination polymers, redox activity has recently deserved special attention. Indeed, mixed valence compounds can show high electronic conduction,^{1–4} whereas solids stable upon redox reactions^{5–7} could lead to enhanced

hydrogen sorption^{8–12} or can be used as anode electrodes for lithium ion batteries,^{13–16} active molds for the preparation of metallic nanoparticles^{8,17–19} and conducting polymers,^{20,21}

*To whom correspondence should be addressed. E-mail: devic@chimie.uvsq.fr.

(1) Takaiishi, S.; Hosoda, M.; Kajiwara, T.; Miyasaka, H.; Yamashita, M.; Nakanishi, Y.; Kitagawa, Y.; Yamaguchi, K.; Kobayashi, A.; Kitagawa, H. *Inorg. Chem.* **2008**, *48*, 9048–9050.

(2) Fuma, Y.; Ebihara, M.; Kutsumizu, S.; Kawamura, T. *J. Am. Chem. Soc.* **2004**, *126*, 12238–12239.

(3) Miyasaka, H.; Motokawa, N.; Matsunaga, S.; Yamashita, M.; Sugimoto, K.; Mori, T.; Toyota, N.; Dunbar, K. R. *J. Am. Chem. Soc.* **2010**, *132*, 1532–1544.

(4) Zeng, M.-H.; Wang, Q.-X.; Tan, Y.-X.; Hu, S.; Zhao, H.-X.; Long, L.-S.; Kurmoo, M. *J. Am. Chem. Soc.* **2010**, *132*, 2561–2563.

(5) Choi, H. J.; Suh, M. P. *J. Am. Chem. Soc.* **2004**, *126*, 15844–15851.

(6) Agusti, G.; Ohtani, R.; Yoneda, K.; Gaspar, A. B.; Ohba, M.; Sanchez-Royo, J. F.; Munoz, M. C.; Kitagawa, S.; Real, J. A. *Angew. Chem., Int. Ed.* **2009**, *48*, 8944–8947.

(7) Ritchie, C.; Streb, C.; Thiel, J.; Mitchell, S. G.; Miras, H. N.; Long, D.-L.; Boyd, T.; Peacock, R. D.; McGlone, T.; Cronin, L. *Angew. Chem., Int. Ed.* **2008**, *47*, 6881–6884.

(8) Cheon, Y. E.; Suh, M. P. *Angew. Chem., Int. Ed.* **2009**, *48*, 2899–2903.

(9) Mulfort, K. L.; Hupp, J. T. *J. Am. Chem. Soc.* **2007**, *129*, 9604–9605.

(10) Mulfort, K. L.; Hupp, J. T. *Inorg. Chem.* **2008**, *47*, 7936–7938.

(11) Dalach, P.; Frost, H.; Snurr, R. Q.; Ellis, D. E. *J. Phys. Chem. C* **2008**, *112*, 9278–9284.

(12) Mulfort, K. L.; Wilson, T. M.; Wasielewski, M. R.; Hupp, J. T. *Langmuir* **2009**, *25*, 503–508.

(13) Férey, G.; Millange, F.; Morcrette, M.; Serre, C.; Doublet, M.-L.; Grenèche, J.-M.; Tarascon, J.-M. *Angew. Chem., Int. Ed.* **2007**, *46*, 3259–3263.

(14) Armand, M.; Grugeon, S.; Vezin, H.; Laruelle, S.; Ribière, P.; Poizot, P.; Tarascon, J.-M. *Nat. Mater.* **2009**, *8*, 120–125.

(15) Xiang, J.; Chang, C.; Li, M.; Wu, S.; Yuan, L.; Sun, J., A. *Cryst. Growth Des.* **2008**, *8*, 280–282.

(16) Chen, H.; Armand, M.; Courty, M.; Jiang, M.; Grey, C. P.; Dolhem, F.; Tarascon, J.-M.; Poizot, P. *J. Am. Chem. Soc.* **2009**, *131*, 8984–8988.

(17) Suh, M. P.; Moon, H. R.; Lee, E. Y.; Jang, S. Y. *A. J. Am. Chem. Soc.* **2006**, *128*, 4710–4718.

(18) Moon, H. R.; Kim, J. H.; Suh, M. P. *Angew. Chem., Int. Ed.* **2005**, *44*, 1261–1265.

(19) Hong, B. H.; Bae, S. C.; Lee, C.-W.; Jeong, S.; Kim, K. S. *Science* **2001**, *294*, 348–351.

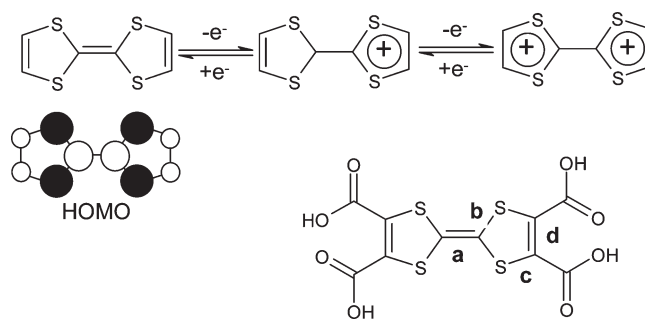
(20) Yanai, N.; Uemura, T.; Ohba, M.; Kadowaki, Y.; Maesato, M.; Takenaka, M.; Nishitsuji, S.; Hasegawa, H.; Kitagawa, S. *Angew. Chem., Int. Ed.* **2008**, *47*, 9883–9886.

(21) Uemura, T.; Kadowaki, Y.; Yanai, N.; Kitagawa, S. *Chem. Mater.* **2009**, *21*, 4096–4098.

or for sensing through guest-network charge-transfer interactions.^{22–24} The electrochemical synthesis of porous coordination polymers by the electrolysis of copper electrodes has also been proposed,^{25,26} and few studies of their electrochemical behaviors have been reported.^{13–16,27} Compared to the purely inorganic porous solids, one noticeable advantage of the coordination polymers is that not only the metallic cations but also suitable organic linkers can act as redox centers.^{8–12,14–16,19,22,23,28}

Tetrathiafulvalene (TTF) derivatives are sulfur-rich π -electron donors known to form organic molecular conducting or even superconducting salts upon partial oxidation (Scheme 1).²⁹ Examples of TTF bearing neutral coordinative groups (N, P or S) are numerous,³⁰ and many coordination complexes have been prepared, mainly with the aim to combine the electronic and magnetic properties of the organic and inorganic moieties in the resulting solids.^{31–38} Few coordination polymers (from 1 to 3-D) have been described,^{34,35,39–46} mostly involving interactions between d¹⁰ cations (Cu, Ag) and sulfur atoms of the TTF backbone.^{34,39,42–44,46} On the other hand, coordination com-

Scheme 1. (Top) Two-Electron Reversible Oxidation of the TTF Core, As Well As the Shape of the Highest Occupied Molecular Orbital (HOMO) and (Bottom) Tetrathiafulvalenetetracarboxylic Acid ((TTF-TC)H₄) Used in the Present Study⁴



^a Letters a–d correspond to the bond distances reported in Table 2.

pounds involving oxygenated anionic binding sites, such as catecholate^{47–50} and carboxylate,^{51–57} are rare and with few noticeable exceptions^{53,55,57} limited to molecular species. This could at first glance appear surprising, since carboxylate linkers are known to afford numerous stable, neutral, and sometimes highly porous 3D coordination networks.^{58–61} The reason for this may be found in the presumed low stability of such linkers, which would make them incompatible with the sometimes harsh (temperature, pH) experimental conditions used for the preparation of stable 3-D coordination polymers. We thus focused our attention on the TTF tetracarboxylic acid⁶² ((TTF-TC)H₄, see Scheme 1), whose characteristics (high symmetry and potentially strong binding site) appear adequate for the preparation of robust 3-D networks. The reactivity of this linker with divalent cations (Ni,Co) was already studied but led to porous hydrogen-bonded networks of isolated carboxylate anions and inorganic cations.^{63,64} For TTF-Co(H₂O)₆(TTF-TC)H₂·2H₂O,⁶⁴ the partial dehydration was thought to give rise to a coordination compound, although this was not structurally evidenced. Only very recently, a 3-D coordination polymer based on Zn, TTF-TC, and 4,4'-bipyridine as a coligand was reported.⁵⁵ Another issue

(22) Shimomura, S.; Matsuda, R.; Tsujino, T.; Kawamura, T.; Kitagawa, S. *J. Am. Chem. Soc.* **2006**, *128*, 16416–16417.
 (23) Shimomura, S.; Horike, S.; Matsuda, R.; Kitagawa, S. *J. Am. Chem. Soc.* **2007**, *129*, 10990–10991.
 (24) Tanaka, D.; Horike, S.; Kitagawa, S.; Ohba, M.; Hasegawa, M.; Ozawa, Y.; Toriumi, K. *Chem. Commun.* **2007**, 3142–4144.
 (25) Mueller, U.; Schubert, M.; Teich, F.; Puetter, H.; Schierle-Arndt, K.; Pastré, J. *J. Mater. Chem.* **2006**, *16*, 626–636.
 (26) Ameloot, R.; Stappers, L.; Fransaer, J.; Alaerts, L.; Sels, B. F.; De Vos, D. E. *Chem. Mater.* **2009**, *21*, 2580–2582.
 (27) Domenech, A.; Garcia, H.; Domenech-Carbo, M. T.; Llabres-i-Xamena, F. J. *Phys. Chem. C* **2007**, *111*, 13701–13711.
 (28) Kitagawa, S.; Kawata, S. *Coord. Chem. Rev.* **2002**, *224*, 11–34.
 (29) See, for example, the special issue on Molecular Conductors: *Chem. Rev.* **2004**, *104*, 4887–5782 and references therein.
 (30) Lorcy, D.; Bellec, N.; Fourmigue, M.; Avarvari, N. *Coord. Chem. Rev.* **2009**, *253*, 1398–1438 and references therein.
 (31) Liu, S. X.; Ambrus, C.; Dolder, S.; Neels, A.; Decurtins, S. *Inorg. Chem.* **2006**, *45*, 9622–9624.
 (32) Lu, W.; Zhang, Y.; Dai, J.; Zhu, Q.-Y.; Bian, G.-Q.; Zhang, D.-Q. *Eur. J. Inorg. Chem.* **2006**, 1629–1634.
 (33) Setifi, F.; Ouahab, L.; Golhen, S.; Yoshida, Y.; Saito, G. *Inorg. Chem.* **2003**, *42*, 1791–1793.
 (34) Ichikawa, S.; Mori, H. *Inorg. Chem.* **2009**, *48*, 4643–4645.
 (35) Ichikawa, S.; Takahashi, K.; Mori, H.; Yamaura, J.-I. *Solid State Sci.* **2008**, *10*, 1724–1728.
 (36) Uzelmeier, C. E.; Smucker, B. W.; Reinheimer, E. W.; Shatruk, M.; O'Neal, A. W.; Fourmigué, M.; Dunbar, K. R. *Dalton Trans.* **2006**, 5229–5268.
 (37) Perruchas, S.; Avarvari, N.; Rondeau, D.; Levillain, E.; Batail, P. *Inorg. Chem.* **2005**, *44*, 3459–3465.
 (38) Geng, Y.; Wang, X.-J.; Chen, B.; Xue, H.; Zhao, Y.-P.; Lee, S.; Tung, C.-H.; Wu, L.-Z. *Chem.—Eur. J.* **2009**, *15*, 5124–5129.
 (39) Ding, Y.; Chen, Q.; Zhong, H.-C.; Munakata, M.; Konaka, H.; Ning, G.-L.; Wang, H.-Z. *Polyhedron* **2008**, *27*, 1393–1400.
 (40) Ichikawa, S.; Kimura, S.; Mori, H.; Yoshida, G.; Tajima, H. *Inorg. Chem.* **2006**, *45*, 7575–7577.
 (41) Jia, C.; Liu, S.-X.; Ambrus, C.; Neels, A.; Labat, G.; Decurtins, S. *Inorg. Chem.* **2006**, *45*, 3152–3154.
 (42) Jia, C.; Zhang, D.; Liu, C.-M.; Xu, W.; Hu, H.; Zhu, D. *New J. Chem.* **2002**, *26*, 490–494.
 (43) Lu, W.; Yan, Z.-H.; Dai, J.; Zhang, Z.; Zhu, Q.-Y.; Jia, D.-X.; Guo, W. J. *Eur. J. Inorg. Chem.* **2005**, 2339–2345.
 (44) Munakata, M.; Kuroda-Sowa, T.; Maekawa, M.; Hirota, A.; Kitagawa, S. *Inorg. Chem.* **1995**, *34*, 2705–2710.
 (45) Olivier, J.; Golhen, S.; Swietlik, R.; Cador, O.; Pointillart, F.; Ouahab, L. *Eur. J. Inorg. Chem.* **2009**, 3282–3290.
 (46) Wu, L. P.; Dai, J.; Munakata, M.; Kuroda-Sowa, T.; Maekawa, M.; Suenaga, Y.; Ohno, Y. *Dalton Trans.* **1998**, 3255–3261.
 (47) Bellec, N.; Massue, J.; Roisnel, T.; Lorcy, D. *Inorg. Chem. Commun.* **2007**, *10*, 1172–1176.
 (48) Massue, J.; Bellec, N.; Chopin, S.; Levillain, E.; Roisnel, T.; Clerac, R.; Lorcy, D. *Inorg. Chem.* **2005**, *44*, 8740–8748.

(49) Xu, C.-H.; Sun, W.; Zhang, C.; Zhou, C.; Fang, C.-J.; Yan, C.-H. *Chem.—Eur. J.* **2009**, *15*, 8717–8721.
 (50) Zhu, Q.-Y.; Bian, G.-Q.; Zhang, Y.; Dai, J.; Zhang, D.-Q.; Lu, W. *Inorg. Chim. Acta* **2006**, *359*, 2303–2308.
 (51) Gu, J.; Zhu, Q.-Y.; Zhang, Y.; Lu, W.; Niu, G.-Y.; Dai, J. *Inorg. Chem. Commun.* **2008**, *11*, 175–178.
 (52) Ebihara, M.; Nomura, M.; Sakai, S.; Kawamura, T. *Inorg. Chim. Acta* **2007**, *360*, 2345–2352.
 (53) Zhu, Q.-Y.; Lin, H.-H.; Dai, J.; Bian, G.-Q.; Zhang, Y.; Lu, W. *New J. Chem.* **2006**, *30*, 1140–1144.
 (54) Faulkner, S.; Burton-Pye, B. P.; Khan, T.; Martin, L. R.; Wray, S. D.; Skabara, P. J. *Chem. Commun.* **2002**, 1668–1669.
 (55) Han, Y.-F.; Li, X.-Y.; Li, J.-K.; Zheng, Z.-B.; Wu, R. T.; Lu, J.-R. *Chinese J. Inorg. Chem.* **2009**, *25*, 1290–1294.
 (56) Pointillart, F.; Le Gal, Y.; Golhen, S.; Cador, O.; Ouahab, L. *Chem. Commun.* **2009**, 3777–3779.
 (57) Wang, J.-P.; Lu, Z.-J.; Zhu, Q.-Y.; Zhang, Y.-P.; Qin, Y.-R.; Bian, G.-Q.; Dai, J. *Cryst. Growth Des.* **2010**, *10*, 2090–2095.
 (58) Férey, G. *Chem. Soc. Rev.* **2008**, *37*, 191–214.
 (59) Yaghi, O. M.; O'Keefe, M.; Ockwig, N. W.; Chae, H. K.; Eddaoudi, M.; Kim, J. *Nature* **2003**, *423*, 705–714.
 (60) Kitagawa, S.; Kitaura, R.; Noro, S.-I. *Angew. Chem., Int. Ed.* **2004**, *43*, 2334–2375.
 (61) Kepert, C. J. *Chem. Commun.* **2006**, 695–700.
 (62) Yoneda, S.; Kawase, T.; Inaba, M.; Yoshida, Z. *J. Org. Chem.* **1978**, *43*, 595–598.
 (63) Han, Y.-F.; Li, M.; Wang, T.-W.; Li, Y.-Z.; Shen, Z.; Song, Y.; You, X.-Z. *Inorg. Chem. Commun.* **2008**, *11*, 945–947.
 (64) Kepert, C. J.; Hesk, D.; Beer, P. D.; Rosseinsky, M. J. *Angew. Chem., Int. Ed.* **1998**, *37*, 3158–3160.

Table 1. Synthesis Conditions of the MIL-132(K), -133(K, Rb), -134(Cs), and -135(K) Solids

solid	(TTF-TC)H ₄ (mmol)	MCl (mmol)	MOH (mmol)	H ₂ O (mL)	temperature (°C)	current density ($\mu\text{A cm}^{-2}$)
MIL-132(K)	0.13	0.26	0.2	3	70	0
MIL-133(K)	0.13	0.26	0.1	3	70	0
MIL-133(Rb)	0.13	0.26	1.2	3	100	0
MIL-134(Cs)	0.13	0.26	1.2	3	100	0
MIL-135(K)	0.13	1.70	0.13	15	70	60

is the redox activity of this linker when included in a coordination polymer. Indeed, coordination compounds based on oxidized TTF ligands are limited.^{31–35,42,45,65–67} This is especially the case for TTF carboxylate derivatives (only one molecular complex reported so far),⁵⁶ which are prone to decarboxylation upon oxidation.⁶⁸

Our aim was thus to examine the ability of the (TTF-TC)H₄ linker to act as an organic building block for the preparation of three-dimensional polymers (porous if possible) and to take advantage of its redox activity in the resulting solid. The first part of this study is devoted to the reactivity of the (TTF-TC)H₄ linker with alkaline ions, which are now considered valuable alternatives to transition metal cations for the preparation of coordination polymers.^{69–73} Four dense 3-D coordination polymers were produced. In a second part, as these compounds were found to be stable, they were tested as positive electrode materials. Indeed, alkaline-based coordination polymers based on redox active linkers were already shown to be promising alternative electrode materials in lithium-ion batteries.^{14–16} Finally, in order to directly prepare coordination polymers based on an oxidized linker, a combined electro-(sub)hydrothermal synthesis was developed. This allows the preparation of a new 3-D solid, which is not based on the neutral TTF-TC however, the oxidized TTF-TC⁺ linker, whose electronic conductivity is studied.

Experimental Section

Synthesis. Tetrathiafulvalenetetracarboxylic acid or (TTF-TC)H₄ was prepared in four steps using a synthesis reported by Pittman et al.;⁷⁴ slight modifications were made to this procedure, which are given in the Supporting Information. Table 1 summarizes the main characteristics of the optimized synthesis conditions of MIL-132(K), MIL-133(K, Rb), MIL-134(Cs), and MIL-135(K), which are fully described in the Supporting Information.

Characterizations. The Supporting Information contains the details of the different techniques (single-crystal and powder X-ray diffraction, thermal analyses (TGA, thermogravimetry), infrared spectroscopy, and liquid cyclic voltammetry) used for the characterization of the solids and the measurement

of their properties (electronic conductivity and reversible and irreversible electrochemical processes).

Results and Discussion

Synthesis, Structure, and Thermal Behavior of the Non-oxidized Solids. Initial reactions of the tetrathiafulvalenetetracarboxylic acid or (TTF-TC)H₄ with potassium salts focused on variations of temperature and pH. It was noted that temperatures exceeding 100 °C resulted in the decomposition of the linker; however, crystalline materials were observed to form below 100 °C. The temperature was then set to 70 °C, and the pH systemically varied: two phases (later called MIL-132(K) and MIL-133(K); MIL stands for Materials Institut Lavoisier) were identified and isolated (see Figure S1, Supporting Information). The same experimental conditions were then transferred to rubidium and cesium. In each case, only one crystalline phase (MIL-133(Rb) and MIL-134(Cs), respectively) was detected throughout the whole pH and temperature range examined. The structures of the four solids were solved by single-crystal XRD (see the Supporting Information); two (K and Rb-based) are isostructural. The four solids correspond to the general formula M₂(TTF-TC)H₂ (M = K, Rb, Cs), which was further confirmed by chemical analysis. In all cases, two of the four carboxylic acid groups are deprotonated, and the remaining hydroxyl groups are involved in strong intramolecular O–H···O hydrogen bonds (see Table S2, Supporting Information, for distances and angles), while the TTF cores are planar and the C–S and C=C bond distances are in accordance with a neutral oxidation state (Table 2).⁷⁵

For MIL-132(K), which was obtained for a wide range of pH's, two clearly distinguishable sets of K–O distances are observed: five short distances between 2.711(2) and 2.795(2) Å and two long ones (2.925(2) Å and 3.017(2) Å). When only considering the short distances, the potassium environment can be described as square pyramidal. In this case, inorganic chains of edge-sharing [KO₅] polyhedra are defined along [010] (K–K = 3.961(1) Å). Two single chains are linked by the carboxylate functions, which remain bidentate and form dimerized single chains (K–K = 4.415(1) Å), whereas the carboxylic acid groups become monodentate, with C–OH dangling groups (Figure 1). Layers of TTF cores parallel to each other with their long axis perpendicular to the layer develop in the 110 plane with their direction alternating along [001] in a herringbone fashion (Figure S10a, Supporting Information). These layers are reminiscent to the β -type slabs found in molecular conductors⁷⁶ but are here built up from uniform 1-D stacks (interplane distance 3.51 Å, shortest S···S distance 3.79 Å) completely isolated from

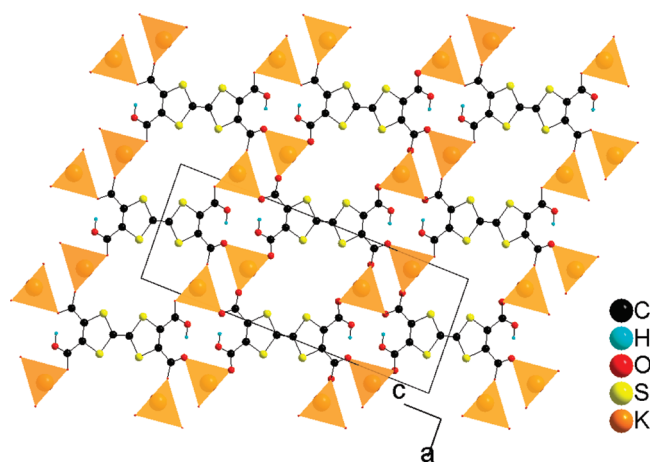
- (65) Avarvari, N.; Fourmigué, M. *Chem. Commun.* **2004**, 1300–1301.
 (66) Hervé, K.; Le Gal, Y.; Ouahab, L.; Golhen, S.; Cadour, O. *Synth. Met.* **2005**, *153*, 461–464.
 (67) Kwon, S.-Y.; Cho, J.-S.; Lee, H.-I.; Lee, U.; Noh, D.-Y. *Inorg. Chim. Acta* **2005**, *8*, 510–512.
 (68) Dolbecq, A.; Fourmigué, M.; Batail, P. *Bull. Chem. Soc.* **1996**, *133*, 83–88.
 (69) Fromm, K. M. *Coord. Chem. Rev.* **2008**, *252*, 856–885.
 (70) Wu, T.; Zhang, J.; Bu, X.; Feng, P. *Chem. Mater.* **2009**, *21*, 3830–3837.
 (71) Banerjee, D.; Kim, S. J.; Borkowski, L. A.; Xu, W.; Parise, J. B. *Cryst. Growth Des.* **2010**, *10*, 709–715.
 (72) Banerjee, D.; Kim, S. J.; Parise, J. B. *Cryst. Growth Des.* **2009**, *9*, 2500–2503.
 (73) Liu, Y.-Y.; Zhang, J.; Xu, F.; Sun, L.-X.; Zhang, T.; You, W.-S.; Zhao, Y.; Zeng, J.; Cao, Z.; Yang, D. *Cryst. Growth Des.* **2008**, *8*, 3127–3129.
 (74) Pittman, C. U.; Narita, M.; Liang, Y. F. *J. Org. Chem.* **1976**, *41*, 2855–2860.

- (75) Guionneau, P.; Kepert, C. J.; Bravic, G.; Chasseau, D.; Truter, M. R.; Kurmoo, M.; Day, P. *Synth. Met.* **1997**, *86*, 1973–1974.
 (76) Mori, T. *Bull. Chem. Soc. Jpn.* **1998**, *71*, 2509–2526.

Table 2. TTF Internal Bond Distances (see Scheme 1 for the definition of a–d) and the Oxidation State of the TTF-TC (Deduced from the Formula) in the Synthesized Solids^a

solid	<i>a</i> (Å)	<i>b</i> (Å)	<i>c</i> (Å)	<i>d</i> (Å)	oxidation state
MIL-132(K)	1.340(5)	1.768(2) 1.764(2)	1.747(2) 1.752(2)	1.360(3)	0
MIL-133(K)	1.353(8)	1.756(2)	1.751(3)	1.353(8)	0
MIL-133(Rb)	1.39(2)	1.751(6)	1.750(7)	1.39(1)	0
MIL-134(Cs)	1.37(1)	1.749(4)	1.746(5)	1.35(1)	0
MIL-135(K)	1.401(5)	1.720(3) 1.728(3)	1.729(3) 1.734(3)	1.359(4)	+1
Co(H ₂ O) ₆ (TTF-TC)H ₂ ·2H ₂ O ⁶⁴	1.335	1.752 1.758	1.745 1.748	1.356	0
[Co ₂ (μ ₂ -OH ₂)(H ₂ O) ₈][(TTF-TC)H ₂] ₂ ·2H ₂ O ⁶³	1.344	1.752 1.744	1.737 1.746	1.350 1.334	0

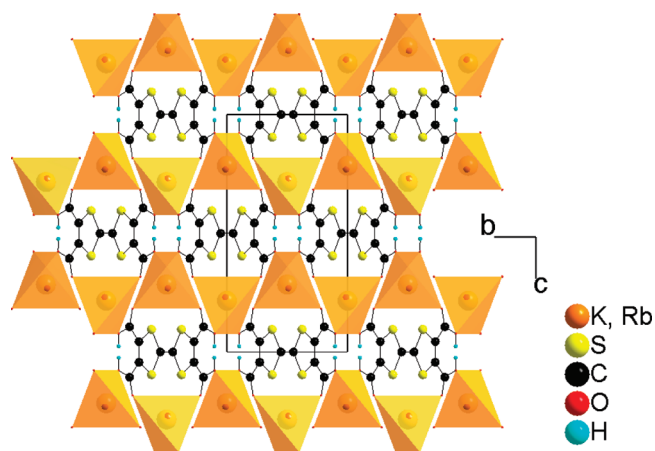
^a For the heaviest cations (Rb, Cs), the large esd's (especially on C=C bonds) mask any clear relation between the bond distances and the oxidation state.

**Figure 1.** Structure of MIL-132(K), projection down [010].

each other (shortest interstack S···S distance > 5.8 Å, see Figure S10b).

If one considers the intermediate pH form (final pH around 3, MIL-133(K)), while keeping the same criterion for K–O distances ($d < 2.85$ Å), four bonds (2.743(2)–2.765(2) Å instead of six when $d < 3.25$ Å) determine a tetrahedral coordination for K. These tetrahedra are not directly linked to each other, but through (TTF-TC)H₂ linkers defining a 3-D network (Figure 2). Hydrogen atoms are distributed on two sites with 50% occupation. Layers of parallel TTF cores with their long axis parallel to the layer develop in the 110 plane, with an alternating orientation down [001]. Each layer is built up from 1-D staggered stacks of TTFs (interplane distance 3.32 Å, shortest S···S distance 3.96 Å) isolated from each other (shortest interstack S···S contact > 6 Å), as shown in Figure S11 (Supporting Information). This finally leads to completely different surroundings of K⁺ ions and whole 3-D networks in the two polymorphs. The solid obtained with rubidium is isostructural to MIL-133(K), and longer Rb–O distances (2.879(6)–2.899(6) Å) lead to only a slight increase of the TTF···TTF distance (shortest interplane distance, 3.37 Å; shortest S···S distance, 3.97 Å).

In the case of cesium (MIL-134(Cs)), the compound crystallizes in a different (monoclinic C-centered cell instead of the orthorhombic primitive) but quite similar structure to those of MIL-133(K, Rb). Indeed, almost identical layers of TTFs (interplane distance, 3.33 Å;

**Figure 2.** Structure of MIL-133(K, Rb) down [100], which is very similar to the [001] projection of MIL-134(Cs).

shortest S···S distance, 3.93 Å) connected through the alkaline cations (Cs–O = 3.086(4)–3.109(5) Å) define the 3-D network (Figure S12, Supporting Information). The structures only differ along the axis of alternation of the organic and inorganic layers (here [010], corresponding to [001] in MIL-133); whereas the direction of the TTFs stacks alternate in MIL-133, it remains unchanged in MIL-134 (Figure 3).

Despite an identical composition (K₂(TTF-TC)H₂), the selective formation of MIL-132 and MIL-133 seems to be driven by the pH; moreover, no thermally induced transition from one polymorph to the other was detected upon heating (see Figure 4). MIL-132(K) has a lower density, and very small 1-D channels (2 × 2.5 Å² taking into account the van der Waals radii) with sulfur-rich walls running along the K–O–K chain axis are observed (see Figure 1). Nevertheless, no significant adsorption (either nitrogen or hydrogen at 77 K) was measured (see Supporting Information). Attempts to grow the same phase with larger cations (Rb, Cs) in order to increase the size of the pores always led to the formation of a dense phase (MIL-133 and MIL-134, respectively).

The thermal stabilities of the solids were evaluated concomitantly by thermogravimetric analysis (under oxygen) and thermodiffraction (under air). Both techniques indicate that the compounds are stable up to 150–200 °C, whatever the nature of the cation; no mass change and structural transformation are observed below

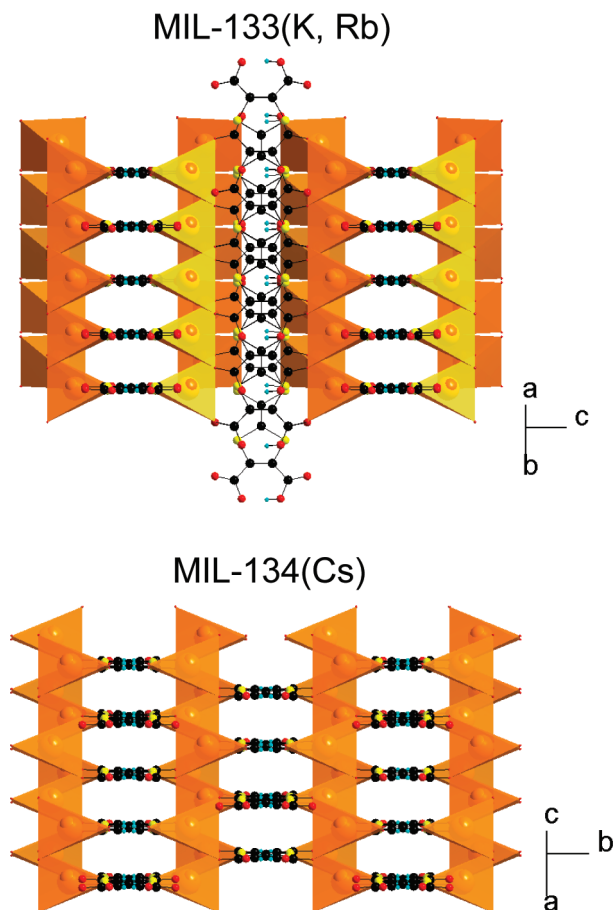


Figure 3. Alternation of inorganic and organic layers in MIL-133(K, Rb) and MIL-134(Cs), illustrating the structural differences between the two solids.

these temperatures (Figure 4). As previously mentioned, no thermally induced structural transition between MIL-132(K) and MIL-133(K) was observed, as can be expected from their largely different crystal structures. Above 200 °C, the solids degrade, eventually yielding crystalline M_2SO_4 ($M = K, Rb, Cs$), with the associated weight losses in accordance with the proposed formula. The thermal stabilities are slightly lower than the ones usually observed in coordination polymers (typically around 300 °C) and could be related to the destruction of the linker, either through (i) irreversible oxidation (see below) or (ii) thermal decarboxylation.

Redox Behavior. The strong tendency of the TTF cores to pack parallel, as seen in MIL-132/134 or in other coordination polymers,⁴¹ could be used to achieve conductivity upon postsynthetic oxidation. Before considering this, it should be noted that, although the TTF core usually presents two reversible oxidation waves, TTF bearing carboxylic moieties are prone to irreversible decarboxylation upon oxidation,⁶⁸ a transformation related to the Kolbe reaction.⁷⁷ Nevertheless, a thorough electrochemical study performed on the TTF monocarboxylic acid suggested that the decarboxylation only occurs during the second oxidation step (i.e., the transformation of the radical monocation to the dication, see Scheme 1), whereas the first oxidation step (from the neutral molecule to the radical monocation) is reversible.⁷⁸ This was recently confirmed by the preparation of a molecular complex of oxidized TTF monocarboxylate.⁵⁶ The same trend was observed by Rosseinsky et al. for $(TTF-TC)H_4$ in water.⁶⁴ Cyclic voltammetry performed in DMF (see Figure S6, Supporting Information) led to the same conclusion, with a first reversible process (the width of the half height corresponds to 60 mV)

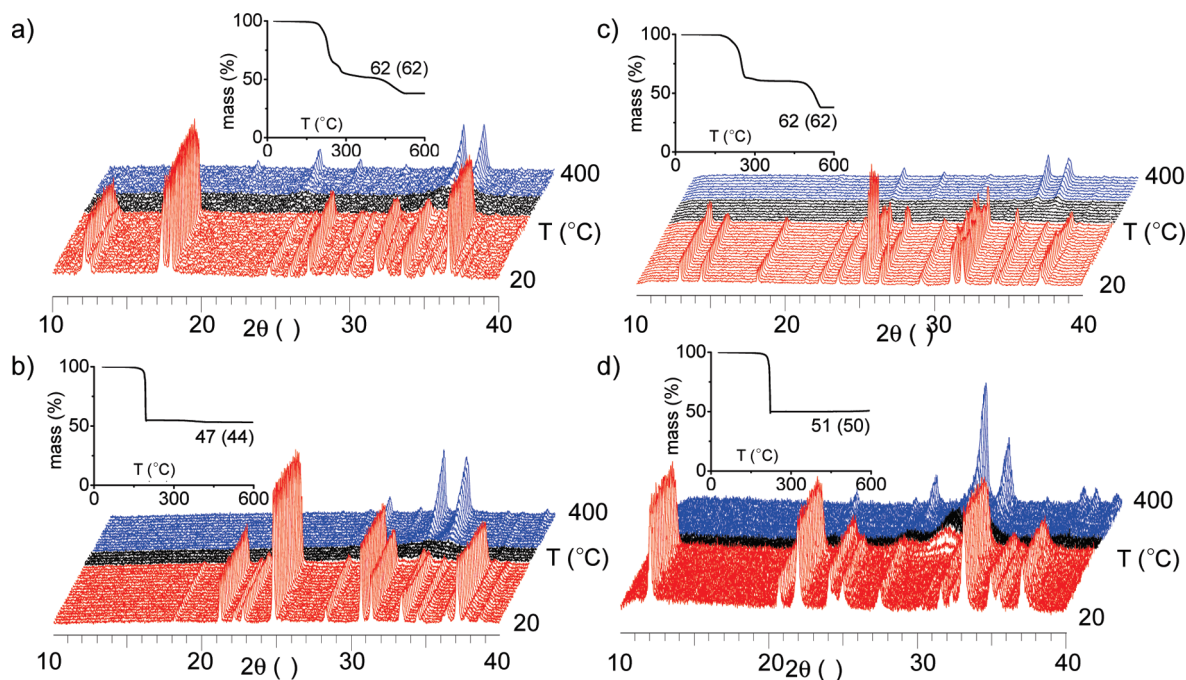


Figure 4. Thermal behavior of the $(TTF-TC)H_2$ -based solids: (a) MIL-132(K), (b) MIL-133(Rb), (c) MIL-133(K), and (d) MIL-134(Cs). Thermo-diffractograms from room temperature to 400 °C: red, as-synthesized solid; black, amorphous intermediate; blue, M_2SO_4 ; $M = K, Rb, Cs$ ($\lambda(\text{CoK}\alpha) = 1.7890 \text{ \AA}$). Inset: Thermogravimetric analysis from room temperature to 600 °C; experimental and theoretical (in parentheses) weight losses are also reported.

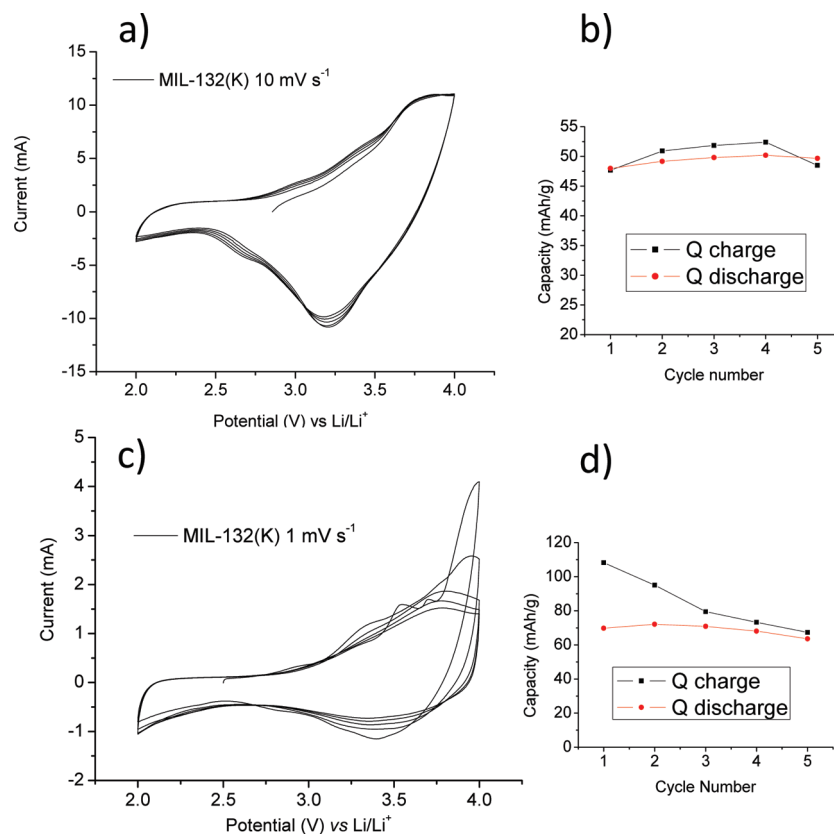


Figure 5. Oxidation behavior of MIL-132(K): (a) solid-state cyclic voltammetry between 2 and 4 V vs Li/Li⁺ at 10 mV s⁻¹, (b) charge/discharge capacities upon cycling between 2 and 4 V vs Li at 10 mV s⁻¹, (c) solid-state cyclic voltammetry between 2 and 4 V vs Li at 1 mV s⁻¹, (d) charge/discharge capacities upon cycling between 2 and 4 V vs Li at 1 mV s⁻¹.

followed by a second irreversible oxidation ($E_{1/2}^1 = 0.53$ V and $E_{1/2}^2 = 0.80$ V vs SCE, respectively).

The direct chemical oxidation of MIL-132(K) and -133(K) was explored initially. Exposure to vapors of iodine or bromine led either to no change (iodine) or to amorphous products (bromine). These results may be explained in terms of relative redox potentials: where iodine is too weak an oxidant to react with (TTF-TC)H₂²⁺, bromine leads to the second, irreversible, oxidation. Electrochemical oxidation, which allows a better control of the redox state, was thus considered. To test the potential applicability of the materials, we investigated the compounds as positive electrode materials in a classical two-electrode Swagelok-type cell using 1 M LiPF₆ containing ethylene carbonate/dimethyl carbonate (EC/DMC) electrolyte, in which metallic lithium foil was used as the negative and reference electrode. Prior to the test, the active materials were hand-milled with 30% w/w Ketjen black carbon (as conductive additives) in an agate mortar.

According to solid-state cyclic voltammogram experiments at different voltage sweep rates, all compounds (MIL-132(K), MIL-133(K), Rb), and MIL-134(Cs)) exhibit a similar behavior. Here, only MIL-132(K) will be discussed in detail (see Figure S7, Supporting Information, for the others). Solid-state cyclic voltammetry

curves of MIL-132(K) at a 10 mV s⁻¹ sweep rate present one highly reversible redox couple (Figure 5a) between 2 and 4 V vs Li/Li⁺, with a charge capacity around 50–60 mAh g⁻¹ (Figure 5b). The reversible charge/discharge processes could be related to the first oxidation of the TTF core (theoretical capacity of MIL-132(K) is 59 mAh g⁻¹ when 1 e⁻ insertion is concerned). At a lower sweep rate (1 mV s⁻¹), at the same voltage range, an irreversible second oxidation of the TTF core is achieved (Figure 5c; theoretical capacity for MIL-132(K) is 118 mAh g⁻¹ when 2 e⁻ insertion is concerned) but which drastically decreased upon cycling and finally reached the value of the first oxidation of the TTF core (Figure 5d). Note that the same irreversible oxidation wave was observed at the solution-state cyclic voltammogram with the TTF tetracarboxylic acid (Figure S6, Supporting Information).

Galvanostatic charge–discharge experiments were performed in order to explore the maximum Li storage ability with a large number of cycles at different current densities and different voltage ranges. Figure 6a shows the charge–discharge profile of MIL-132(K) with a 10 C rate (which corresponds to the current required to completely charge/discharge an electrode in 6 min) at potential values between 2.3 V and 3.75 V. The curve presents continuous dependence on the potential versus composition that can be assessed to a typical solid solution reaction where reversible 0.6 e⁻ insertions were clearly observed. Rate performance (Figure 6b) also depicted the highly reversible capacity of MIL-132(K) at both 10 and 2 C. Initially, the cell was cycled at a 10 C rate, and the potential was increased stepwise to 3.8 V where the

(77) See for example: Grimshaw, J. *Electrochemical reactions and mechanisms in organic chemistry*; Elsevier: Amsterdam, The Netherlands, 2000.

(78) Idriss, K. A.; Chambers, J. Q. *J. Electroanal. Chem.* **1980**, *109*, 341–352.

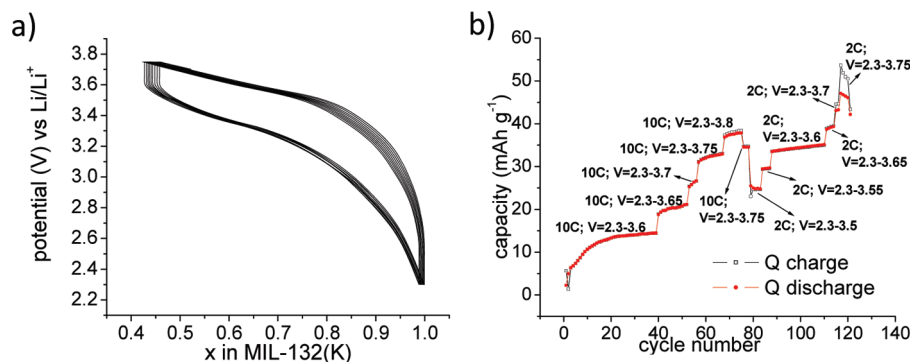


Figure 6. (a) Galvanostatic charge–discharge profile of MIL-132(K) at constant 10 C current density for the voltage range between 2.3 and 3.75 V. (b) Rate performance of MIL-132(K) at both 10 and 2 C with different voltage ranges.

capacity reached 40 mAh g^{-1} . The reversibility is demonstrated by the fact that the capacity is reached again once the potential is lowered to 3.75 V. At a slightly lower C rate (herein 2 C), irreversible capacity loss should not be neglected in the voltage range 2.3–3.7 V, which is presumably due to the decarboxylation of the carboxylic acid groups, as is known to happen during the second oxidation step.

In such a system, oxidation of the molecule backbone requires additional anion insertion (from the electrolyte; PF_6^-) or departure of the cations (from the structure; K^+ , Rb^+ , or Cs^+) in order to maintain the electroneutrality of the structure. Herein, this phenomenon is still not clear, although the structure turns out to be a completely amorphous phase after charge–discharge processes. Also, a clear structural change is observed when the material (e.g., MIL-132(K)) is contacted with the electrolyte, resulting in a badly crystallized structure (Figure S8, Supporting Information). This phenomenon of an electrolyte effect as well as a better understanding of the role of irreversible capacity loss at low rates ($< 2 \text{ C}$) are ongoing studies in our laboratories and will be a subject for another upcoming paper.

However, even considering the unanswered questions surrounding the electrochemical studies, the promising capacities at high-rate performances must be underlined. It is also really important to stress that these new compounds are synthesized in their reduced state (discharge state of a positive electrode). Thus, they are compatible with Li-ion technology since they will provide their electrons during the first charge. Moreover, the average potential, 3.6 V, versus lithium is also comparable or even higher than that of other inorganic compounds (e.g., LiFePO_4). Indeed by comparison with the conventional inorganic cathode materials such as LiFePO_4 or LiCoO_2 (unless further modified), the new TTF based 3D organic frameworks are beneficial electrode materials especially when high-current-regime-required purposes are concerned.

Electrocrystallization. Electrocrystallization is often considered the method of choice for the preparation of crystalline TTF radical salts, allowing both a high purity and a good reproducibility.⁷⁹ Nevertheless, as already stated,³⁰ the use of this technique for the preparation of complexes based on *oxidized* TTF derivatives is rather

limited,^{33,45,65,66} chemical oxidation being the preferred method.^{31,32,34,35,42,56,67} A plausible reason could be the lower stability of the complexes once the TTF-based ligands are oxidized. Indeed, whereas chemical oxidation often allows simultaneous coordination and oxidation processes to occur (for example, using Cu(II) as both a metal and oxidant source^{32,34,35,67}), the electrocrystallization is performed on presynthesized complexes^{33,65,66} (except in one recent case⁴⁵). Indeed, formation of crystalline products which could require a “high” temperature is usually not accessible using conventional electrocrystallization setups. This problem could be circumvented by the combination of electrocrystallization and solvothermal techniques. Coupled electro-hydrothermal systems were developed, mainly for the preparation of polycrystalline films,^{80–89} rods,⁹⁰ or single crystals of oxides.^{91–93} We used here the same technique for the preparation of crystalline coordination polymers based on *oxidized* linkers. Using an autoclave equipped with two platinum electrodes, we were able to directly transfer the experimental conditions used for the preparation of MIL-132(K) and MIL-133(K) to our galvanostatic electrocrystallization experiments.

Whereas at pH's higher than 3 only a small amount of MIL-132(K) is observed, experiments performed at a low pH (1.5–3) produce a black crystalline solid on the anode (later denoted MIL-135(K)), presenting an XRD powder

(80) Ban, S.; Maruno, S. *J. Biomed. Mater. Res. A* **1998**, *42*, 387–395.

(81) Han, K.-S.; Krtil, P.; Yoshimura, M. *J. Mater. Chem.* **1998**, *9*, 2043–2048.

(82) Kajiyoshi, K.; Sakabe, Y. *J. Am. Ceram. Soc.* **1999**, *82*, 2985–2992.

(83) Kajiyoshi, K.; Yanagisawa, K. *J. Phys.: Condens. Matter* **2004**, *16*, S1351–S1360.

(84) Kajiyoshi, K.; Yanagisawa, K.; Feng, Q.; Yoshimura, M. *J. Mater. Sci.* **2006**, *41*, 1535–1540.

(85) Lee, Y.; Watanabe, T.; Takata, T.; Kondo, J. N.; Hara, M.; Yoshimura, M.; Domen, K. *Chem. Mater.* **2005**, *17*, 2422–2426.

(86) Watanabe, T.; Cho, W.-S.; Suchanek, W. L.; Endo, M.; Ikuma, Y.; Yoshimura, M. *Solid State Sci.* **2001**, *3*(1–2), 183–188.

(87) Yoshimura, M.; Suchanek, W. *Solid State Ionics* **1997**, *98*, 197–208.

(88) Yoshimura, M.; Suchanek, W.; Han, K.-S. *J. Mater. Chem.* **1999**, *9*, 77–82.

(89) Yoshimura, M.; Urushihara, W.; Yashima, M.; Kakihana, M. *Intermetallics* **1995**, *3*, 125–128.

(90) Park, S. K.; Park, J. H.; Ko, K. Y.; Yoon, S.; Chu, K. S.; Kim, W.; Do, Y. R. *Crys. Growth Des.* **2009**, *9*, 3615–3620.

(91) Liu, L.; Wang, X.; Bontchev, R.; Ross, K.; Jacobson, A. J. *J. Mater. Chem.* **1999**, *9*, 1585–1589.

(92) Wang, X.; Liu, L.; Bontchev, R.; Jacobson, A. J. *Chem. Commun.* **1998**, 1009–1010.

(93) Wang, X.; Liu, L.; Jacobson, A. J.; Ross, K. *J. Mater. Chem.* **1999**, *9*, 859–861.

(79) Batail, P.; Boubekur, K.; Fourmigué, M.; Gabriel, J. C. P. *Chem. Mater.* **1998**, *10*, 3005–3015.

pattern different from those of both MIL-132(K) and MIL-133(K) (see Figure S3, Supporting Information). The optimization of the experimental parameters (pH and current density, see Figure S2, Supporting Information) afforded a solid suitable for single-crystal analysis. One can note that this optimized current density is higher (about 10 times) than the one usually used for the preparation of TTF-based molecular materials at ambient temperature, which could be related to the higher solubility and diffusion rate of the precursors at high temperatures (here, 70 °C).

The structural resolution reveals a 1:1 TTF-TC/K stoichiometry. The linker adopts the diprotonated state previously observed in the other solids ((TTF-TC) H_2), including the formation of strong intramolecular O–H···O hydrogen bonds (see Table S2, Supporting Information). When compared with MIL-132(K) and MIL-133(K), the internal C–S and C=C bond distances respectively decrease and increase, as expected from the shape of the HOMO when oxidation of the TTF core occurs (see Table 2 and Scheme 1).⁷⁵ The solid could thus be formulated K(TTF-TC $^{+}$) H_2 . The TTF-TC core is shown to be oxidized, but not decarboxylated, as anticipated from cyclic voltammetry measurements.

If one takes into account the same criterion for K–O distances as the one used to describe MIL-132(K) and MIL-133(K), the potassium cations appear to be six-coordinated (K–O = 2.707(2)–2.823(2) Å) in a slightly distorted octahedral environment. They are not directly connected to each other but through bridging carboxylate groups down [100] to define chains. These chains arrange in layers in the 001 plane, alternating down [001] with organic slabs (Figure 7) to finally define a 3-D coordinated network.

The organic layers of (TTF-TC) H_2 are once again reminiscent of the β -type topology found in molecular conductors, i.e., built up from *uniform* 1-D stacks of TTF (interplane distance, 3.45 Å; shortest S···S distance, 3.66 Å) closer to each other (shortest interstack S···S contact is 3.76 Å along [010]) than in MIL-132(K) (see Figure 9a and b). Nevertheless, if one compares the arrangement of the oxidized TTF in MIL-135(K) and in typical molecular conductors, some differences emerge. Whereas the packing of the TTF cores is mainly driven by the optimization of the HOMO–HOMO overlap in molecular conductors (and in some cases additional supramolecular interactions such as hydrogen bonds),⁹⁴ the intrinsic rigidity afforded by the coordination of the inorganic cation constrains, at least partially, the packing of the TTF cores. Indeed, although fully oxidized TTFs (+1 oxidation state) usually tend to form an eclipsed dyad to maximize the HOMO–HOMO overlap,⁹⁵ the packing observed in MIL-135(K) corresponds only to a poor overlap (see Figures 9b and Figure S13, Supporting Information).

The thermal behavior of MIL-135(K) was investigated using the same conditions as those used for the solids based on the nonoxidized (TTF-TC) H_2 linker. This solid

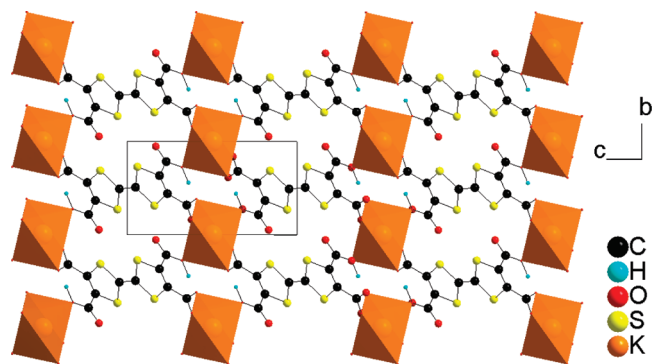


Figure 7. Structure of K(TTF-TC $^{+}$) H_2 or MIL-135(K), projection down [100].

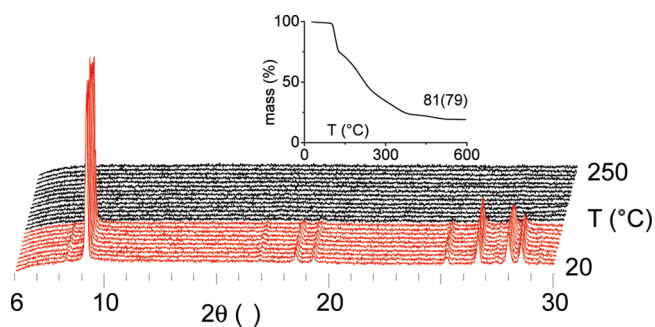


Figure 8. Thermal behavior of MIL-135(K). Thermodiffractogram from room temperature to 250 °C; red, as-synthesized solid; black, amorphous intermediate ($\lambda(\text{CoK}\alpha) = 1.7890$ Å). Inset: Thermogravimetric analysis from room temperature to 600 °C; experimental and theoretical (in parentheses) weight losses are also reported.

is rigid and stable up to about 100 °C and is thermally destroyed above this temperature to give K $_2$ SO $_4$ (Figure 8), with a weight loss in agreement with the proposed formula. Compared to MIL-132(K) and MIL-133(K), MIL-135(K) thus presents a lower thermal stability, which is probably related to the higher reactivity of the oxidized TTF-TC $^{+}$ core.

Finally, the electronic conductivity of a single crystal of MIL-135(K) was investigated from room temperature to 180 K and is shown in Figure 9c. The solid exhibits a semi-conducting behavior with a rather low room-temperature conductivity ($\sigma_{RT} \sim 1 \text{ mS cm}^{-1}$) in comparison with molecular TTF-based materials and an activation energy of 2400 K (0.22 eV). This result is not completely unexpected considering the oxidation state of the TTF core (+1) and the bad TTF···TTF overlap, which prevent an efficient electronic delocalization along the stacks of TTF molecules (see Figures 9a and b).

Conclusion

The use of (TTF-TC) H_4 as an organic building block for the preparation of 3-D coordination polymers was investigated. Although this linker appears less stable than the commonly used hydrocarbonated polycarboxylates, the synthesis of coordination polymers is achievable, providing that some precautions are taken into account, mainly in terms of temperature and pH of the reaction mixture. The reaction of (TTF-TC) H_4 with alkaline ions indeed led to four 3-D solids formulated M $_2$ (TTF-TC) H_2 (M = K, Rb, Cs)

(94) Fourmigué, M.; Batail, P. *Chem. Rev.* **2004**, *104*, 5379–5418.

(95) Devic, T.; Domercq, B.; Auban-Senzier, P.; Molinié, P.; Fourmigué, M. *Eur. J. Inorg. Chem.* **2002**, 2844–2849.

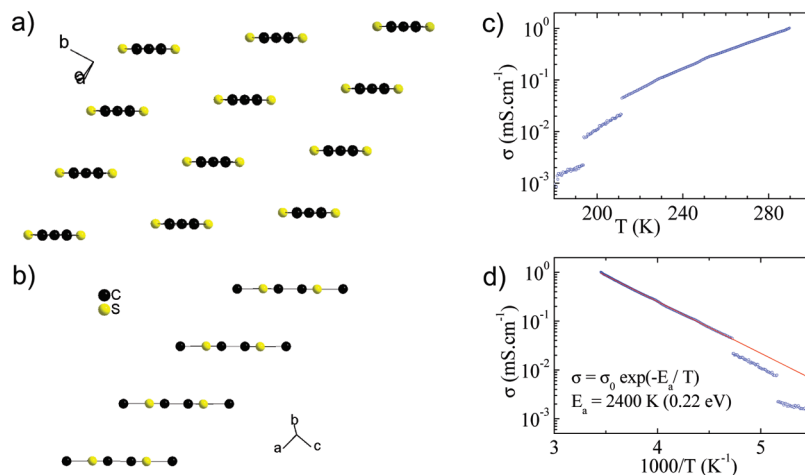


Figure 9. Left: Organic part in MIL-135(K): (a) View of the organic slab along the long axis of the TTFs molecules, reminiscent of a β layer in the 110 plane; (b) view of the uniform 1-D stack along the short axis of the TTF molecules (carboxylate groups are omitted for clarity). Right: (c) temperature dependence of the electronic conductivity of MIL-135(K); (d) fit of the data to a law of the type $\sigma = \sigma_0 \exp(-E_a/T)$.

crystallizing in three different structure types. All the solids demonstrated a reasonable thermal stability in the air but no permanent porosity. They were shown to act as positive electrode materials in lithium batteries exhibiting good cyclabilities. Although the capacities are still moderate with regard to fulfilling lithium batteries market requirements, the TTF-based redox-active compounds are promising potential materials, especially at high current densities. Finally, the direct synthesis of coordination polymers based on the *oxidized* TTF-TC was investigated using a combined electrocrystallization–(sub)hydrothermal approach. This technique allows the preparation of a new compound formulated $\text{K}(\text{TTF-TC}^+)\text{H}_2$ in which the TTF core is oxidized while maintaining its molecular integrity. This dense solid exhibits a semiconducting behavior. Further work will mainly be driven by the use of transition metals in place of alkaline ions

and the development of the combined electrocrystallization–hydrothermal approach in the prospect of producing truly conductive, multifunctional, porous coordination polymers.

Acknowledgment. The authors acknowledge the MENRT and the ANR for financial support (Ph.D. grant for T.L.A. N. and project “CONDMOFs”, respectively), the ESRF for providing access to the beamline BM01A, Dr. N. Avarvari for providing some organic precursors, Dr. S. Miller for his help in hydrogen sorption experiments, and Pr. C. Pasquier for fruitful discussions.

Supporting Information Available: Full synthetic procedures, characterization, and complete XRD data (experimental details, structural description, cif files). This material is available free of charge via the Internet at <http://pubs.acs.org>.